Davey-Stewartson 方程式の局在解の安定性について

東大工　西成活裕　(Katsuhiro Nishinari)

東大工　矢嶋徹 (Tetsu Yajima)

1. Introduction

Localized structures in multidimensions are one of the recent interests for researchers in various fields. They are worth studying both from a theoretical and a practical point of view. Dromion[1] is one of the examples of such structures which appears in the system described by the Davey-Stewartson (DS) 1 equations[2]

$$iA_t + A_{xx} + A_{yy} - 2|A|^2A + (Q_x + Q_y)A = 0, \tag{1}$$

$$Q_{xy} = |A|_x^2 + |A|_y^2. \tag{2}$$

One of the characters of the dromion solutions to emphasize is that the main flow A is localized in two-dimensional space, while the mean flow Q is not. The mean flow is driven at the boundaries like one-dimensional soliton[3], and plays an important role on conveying the localized structures of the main flow[3],[4]. The DS1 equations are derived in many branches of physics, such as fluid dynamics[5] or plasma physics[6]. The stability of dromions can assure us observation of localized structures in real multi-dimansional systems. In our previous paper[7], we have analyzed the time evolutions of the dromion solutions numerically. We have shown that a single dromion propagates stably in the Lyapunov sense, and that in a special case of a collision of two dromions, the initial dromions break into four stable pulses after the collision. This paper is devoted to the numerical analysis of the stability of dromions against their collisions in detail. Speaking of the appearance of four stable pulses in the final stages, the exact (2,2)-dromion solutions also show that dromions are annihilated or created due to collisions, where the no-

tation (M, N)-dromion solution represents the solution which has asymptotically M mean flows in $y = -\infty$ and N in $x = -\infty$. These exact solutions are close to our configuration. It should be noted, however, that our cases are different from exact (2,2)-dromion solutions, since the boundary conditions of the mean flows in our simulations are different from the exact ones.[7] Since little is known about behaviors of the solutions which deviate from exact ones, it is significant to carry out numerical simulations and clarify the behaviors of the collisions of two one-dromions.

We would like to emphasize that the Lyapunov analysis[8] cannot be used to investigate the stability of the dromion solutions. This analysis is applicable only when the equation in consideration has a Hamiltonian. The stability of localized pulses is studied in detail by this method in the case of the nonlinear Schrödinger equation. To the contrary, for the dromion solution of the DS1 equations, we cannot construct the Hamiltonian (Appendix). This is why we investigate the stability numerically in this paper.

The outline of this paper is as follows. In Sec.2, we briefly explain the numerical method and boundary conditions of the simulation. In Sec.3, numerical results of collisions of dromions in various cases are presented and concluding remarks are given in Sec.4.

2. The one-dromion solution and the numerical method

   2.1 The one-dromion solution

Let us summarize the one-dromion solution of the DS1 equations. Eqs. (1) and (2) can be rewrited in another form:

$$iA_t + A_{xx} + A_{yy} + (U + V)A = 0, \tag{3}$$

$$U_y = (|A|^2)_x , \qquad V_x = (|A|^2)_y , \tag{4}$$

where $U = Q_x - |A|^2$ and $V = Q_y - |A|^2$. The one-dromion solution is given by[4]

$$A = \frac{G}{F},\tag{5}$$

here we choose

$$\left.\begin{array}{l} F = 1 + \exp(\eta_1 + \eta_1^*) + \exp(\eta_2 + \eta_2^*) + \gamma \exp(\eta_1 + \eta_1^* + \eta_2 + \eta_2^*), \\[2mm] G = \rho \exp(\eta_1 + \eta_2). \end{array}\right\}\tag{6}$$

The parameters in (6) are given as

$$|\rho| = 2\sqrt{2k_r l_r (\gamma - 1)}$$

$$\eta_1 = (k_r + ik_i)x + (\Omega_r + i\Omega_i)t, \qquad \eta_2 = (l_r + il_i)y + (\omega_r + i\omega_i)t,$$

$$\Omega_r = -2k_r k_i, \qquad \omega_r = -2l_r l_i, \qquad \omega_i + \Omega_i = k_r^2 + l_r^2 - k_i^2 - l_i^2,$$

where constants γ, k_r, k_i, l_r and l_i are real and we take Ω_i as $1/2$ in this paper. There are five substantial free parameters in the dromion solution. The constant γ determines an amplitude, k_r the width of the pulse in the x-direction and l_r that in the y-direction. The quantities k_i and l_i are x and y components of velocity, respectively.

Potentials U and V are determined by integrating (4), and we obtain

$$U = 2(\ln F)_{xx}, \qquad V = 2(\ln F)_{yy}.\tag{7,8}$$

From (7) and (8), we can get the cross section of U and V at the boundary $y, x = -\infty$, respectively:

$$U|_{y=-\infty} = \frac{8k_r^2 \exp(\eta_1 + \eta_1^*)}{(1 + \exp(\eta_1 + \eta_1^*))^2},\tag{9}$$

$$V|_{x=-\infty} = \frac{8l_r^2 \exp(\eta_2 + \eta_2^*)}{(1 + \exp(\eta_2 + \eta_2^*))^2}.\tag{10}$$

It is crucial for the dromion solution driving the potentials from boundaries as (9) and (10).

2.2 Numerical method

Next, we describe the numerical method briefly. We carry out the computation in a region $[-p,p]\times[-p,p]$, where this means the area $|x| \leq p$ and $|y| \leq p$ in the xy-plane. This area is transformed into $[0,2\pi]\times[0,2\pi]$ by transformations of variables $x \rightarrow \pi(x+p)/p$ and $y \rightarrow \pi(y+p)/p$. We take p as 15 throughout simulations, and the grid has been taken 64×64. The space derivatives in (3) has been performed by using the psudospectral method with periodic boundary condition. Time integration is performed by both the Burilsh and Store method [9] and the fourth order Runge-Kutta method with appropriate accuracy of adaptive step size control. The equation (4) is calculated by the fourth order Runge-Kutta method with boundary conditions (9) and (10). We use cubic spline when the midpoint value between meshes is needed. We evaluate the first conserved quantity $I_1 = \int |A|^2 dv$ with appropriate accuracy.

Finally, let us examine the accuracy of using the boundary conditions (9) and (10) in these simulations. In an exact sense, because the simulations have been performed in the region $[-p,p]\times[-p,p]$, we must choose the value of $U(x,y=-p)$ as the boundary conditions of U and $V(x=-p,y)$ as that of V, respectively. The functions of (9) and (10), however, is useful in a practical sense because of its simplicity. Of course the two conditions are identical if we could take $p=\infty$. Hereafter in this paper, we choose the cross sections (9) and (10).

3. Results of simulations

In this section, we present the numerical results of the collision of single dromions. We take superpositions of the two one-dromion solutions as initial conditions. It is obvious that these cannot be exact solutions of this nonlinear equations, since we take only superpositions of a single dromion solution.

To start with, we study by changing the relative velocity with keeping the mass ratio as 1 and the impact parameter as zero (i.e. head-on collisions of two identical dromions in various relative velocities). We take $k1_r = k2_r = l1_r = l2_r = 0.8$ and $\gamma 1 = \gamma 2 = 3.0$, and we choose the following cases for the velocities:

$$(k1_i, k2_i, l1_i, l2_i) = (W/8, -W/8, W/8, -W/8), \qquad W = 3, 4, 5, 6.$$

We see that the constant of motion $I_1 = \int |A|^2 dv$ have been conserved with high accuracy in all of the computations reported here (maximum fluctuation of I_1 during calculation is at most $\Delta I_1 / I_1 \sim 10^{-15}$).

The collision for $W = 5$ is shown in Fig.1. These figures show the typical aspects of the collision. As two dromions approach each other, both of them emit their parts and a third pulse is formed midway between them. The pulse becomes higher and flat on $x = -y$, while two dromions become smaller (Fig.1(b) and (c)). These dromions remain as small side pulses. In the next stage, the side pulses approach each other and become larger again crawling the midway pulse (fig.1(d)). Then, the midway pulse becomes smaller and two pulses on $x = y$ become larger. We can observe two small lumps appear on $x = -y$, which are the remainders of edges of the midway pulse(fig.1(e)). Finally, the two lumps become larger and there appear four pulses. These four pulses gradually separate away and propagate almost stably(Fig.1(f) and (g)). There are also small ripples of the main flow along potentials U and V. The amplitudes of the ripples are less than 8% of the heights of pulses. We find that the two pulses on $x = -y$ are similar. It should be noted that the aspects of the collision are highly symmetrical with respects to $x = y$ throughout the calculations. Theoretically speaking, this system has this symmetry, and the results of the simulation agree with this.

The reason that four pulses appear in the final stage can be understood as follows. Figs.2,3,4 and 5 are the contour plots of the quantities A, U and V

during the collisions with different relative velocities. It is observed that the four pulses are located around the cross points of U and V, where the peaks of the potentials overlap. Considering (3) and (4), we easily see that the potentials U and V are attractive in this case. Then the cross points of them are the most attractive points in the entire region. This explains the fact that the cross points of potentials attract main flow A, and it is natural that four pulses appear after collision.

It is interesting to note here that the two on $x = y$ are bigger than those on $x = -y$ in the cases of figs.2 and 3, although in the cases of figs.4 and 5 the two on $x = -y$ are bigger than that on $x = y$. Let us explain this phenomenon in detail.

From these figures, especially from Fig.5, the large midway pulse on the origin oscillates between two states: a pulse flat in the direction along $x = y$ and that along $x = -y$. This oscillation occurs during the period that the two pulses of U and those of V are sufficiently close, respectively. We can evaluate the periods of the oscillations from these figures. The periods do not change remarkably in all of these cases, the half of them, $T/2$, is $1 \sim 1.5$. Thus we think that the period may be irrelevant to the relative velocity. In order to examine this assertion we simulate the collision with the velocities $(k1_i, k2_i, l1_i, l2_i) = (1/8, -1/8, 1/8, -1/8)$ (Fig.6). We observe that the midway pulse oscillates during four periods of it, and confirm the universal nature of the oscillation that the half period of each oscillation is $1 \sim 1.5$.

This oscillation plays an important role in the final stages of collisions. Before the collision, we observe four common points of the peaks of the mean flow, which play a role of attracting point. As these four points approach, a strong attractive point is formed around the origin. Then, since structures of the main flow are attracted to this point, some parts of the dromions flow into the area around

the origin to form the midway pulse. The new pulse is strongly bounded to the attractive point, so that it oscillates because of the inertia of the fluid. When the pulses of the mean flows sufficiently separate away in the course of time, the attracting point at the origin will be divided again into four intersections of the mean flows. The oscillation stops at this stage and the midway pulse is separated into four, each of which is located at the intersections of the mean flows. Therefore, the timing of the separation of the potentials determines "how initial two dromions break into four pulses in the final stage of their collision."[7] We call this mechanism as "the distribution law" in this paper. In Figs.2 and 3, the potentials separate when the midway pulse is flat along $x = y$, then as a result the two pulses on $x = y$ are larger than the other two in their final stages. The situations in Figs.4 and 5 are opposite to those in Figs.2 and 3. Thus we have explained the differences in the final stages.

Next, we carry out numerical simulations under other conditions, by changing the impact parameter slightly from zero and the mass ratio slightly from unity. We can conclude by the numerical results that a small impact parameter does not affect the aspects of the collision. We then change the mass ratio slightly from unity. In this case the initial dromions exchange their masses each other through the interaction, breaking into four pieces.

4. Concluding remarks

In this paper, collisions of dromions are studied in detail numerically. We confirm that in general, the initial two dromions will break into four pulses after collisions. This holds even if we make small changes on the mass ratio and the impact parameter. The four pulses in the final stage are located around the cross point of the potentials, the area where the peaks of the mean flows inter-

sect, and these intersections are the most attractive points in this system. We also observe the new phenomena that the intermediate pulse created due to collision shows an oscillation during the potentials overlap sufficiently. The pulse is observed to oscillate on between two states, the directions along which they are flat are completely different. One of the remarkable feature of the oscillation is that the period is independent of the relative velocity. Moreover, we find that the state of the oscillation and the relative velocity determine the distribution of total mass into four in the final stage. At present, we think that it is difficult to explain the distribution law by using exact (2,2)-dromion solutions. Therefore, it will be considered that the law is essentially new one.

Appendix

In this Appendix, we discuss the problem of constructing the Hamiltonian of the DS1 equations for the dromion solution. For sufficiently localized pulses of A and Q, we can get eqs. (1) and (2) from variational problems:

$$\frac{\delta H}{\delta A^*} = iA_t, \tag{A.1}$$

$$\frac{\delta H}{\delta Q} = 0, \tag{A.2}$$

where the Hamiltonian is

$$H = \int (|A_x|^2 + |A_y|^2 + |A|^4 - (Q_x + Q_y)|A|^2 + \frac{Q_x Q_y}{2})dV. \tag{A.3}$$

In the calculation of the variation in eqs. (A.1) and (A.2), surface terms must vanish to obtain the DS1 equations. When we consider a dromion solution, the variable A decays exponentially in all the direction. Then all of the surface terms disappear in the variation (A.1) and we obtain (1). On the other hand, we cannot succeed in having the eq.(A.2) because the function Q is not localized. In calculating the left-hand side of (A.2), the variation of the last term in (A.3) is

$$\delta \int \frac{1}{2} Q_x Q_y dV = \frac{1}{2} \int B_Q^{(x)} dy + \frac{1}{2} \int B_Q^{(y)} dx - \int Q_{xy} \delta Q dV.$$
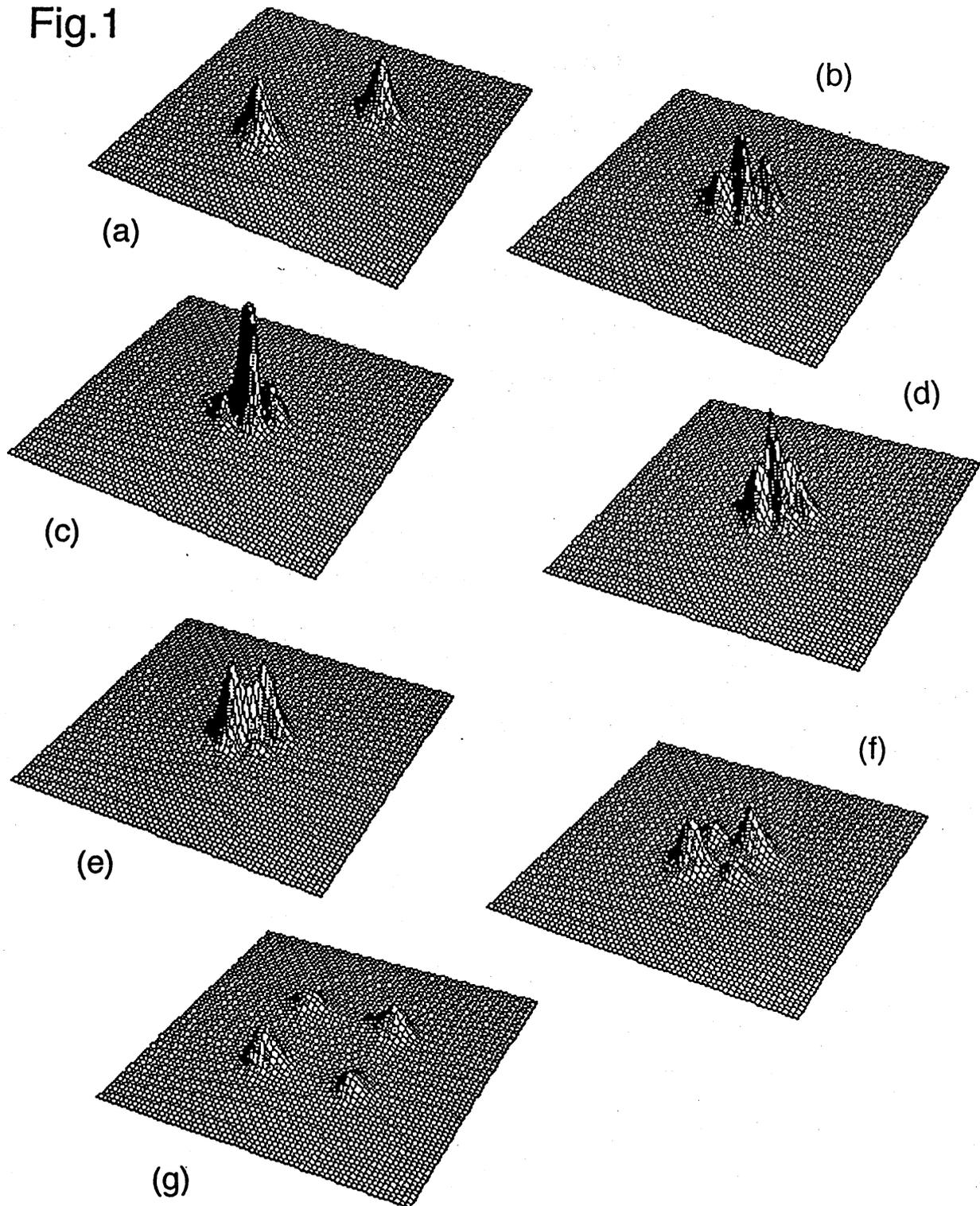
$$B_Q^{(x)} \equiv [Q_y \delta Q]_{x=-\infty}^{x=\infty}, \qquad B_Q^{(y)} \equiv [Q_x \delta Q]_{y=-\infty}^{y=\infty} \qquad (\text{A.4})$$

The first two terms of the right-hand side of (A.4) must vanish to get a non-trivial Hamiltonian. This occurs only when the cross sections of Q at $x = +\infty$ and $y = +\infty$ coincide with those at $x = -\infty$ and $y = -\infty$, respectively. However, it is easily seen that these conditions are not satisfied in the case of the dromion solution, because it is not symmetrical with respects to x and y axes. Thus we cannot construct the Hamiltonian in this case. Consequently, the Lyapunov analysis is not applicable to examine the stability of dromion. This fact is quite natural from the physical point of view.[7] A dromion is located at a cross point of the peaks of two mean flows, We have to drive these mean flows from boundaries of a system. From this reason, this system has an energy interaction with an external system through its boundaries. Therefore, it is apparent that this system is not a Hamilton system.
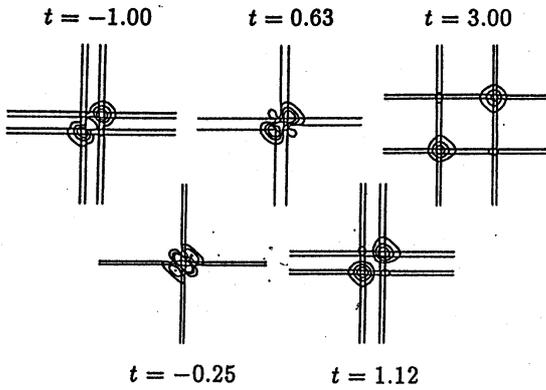
References

[1] M. Boiti, J. J.-P. Leon, L. Martina and F. Pempinelli, Phys. Lett. A **132** (1988) 432.

[2] M. J. Ablowitz and H. Segur, *Solitons, and the Inverse scattering transform* (SIAM, Philadelphia, 1981), p. 322.

[3] A. S. Fokas and P. M. Santini, Phys. Rev. Lett. **63** (1989)1329.

[4] J. Hietarinta and R. Hirota, Phys. Lett. A **145** (1990) 237.

[5] A.Davey and K.Stewartson, Proc. Roy Soc. Lond. A **338** (1974) 101.

[6] K. Nishinari, K. Abe and J. Satsuma, Phys. Plasmas, **1** (1994) 2559.

[7] K. Nishinari and T. Yajima, to appear in J.Phys.Soc Jpn.

[8] E. A. Kuznetsov, A. M. Rubenchik and V. E. Zakharov, Phys. Rep. **142**, No.3 (1986) 103.

[9] W. H. Press, B. P. Flannery, S. A. Teukolsky and W. T. Vetterling, *Numerical Recipes in C* (Cambridge University Press, London, 1992), p. 722.
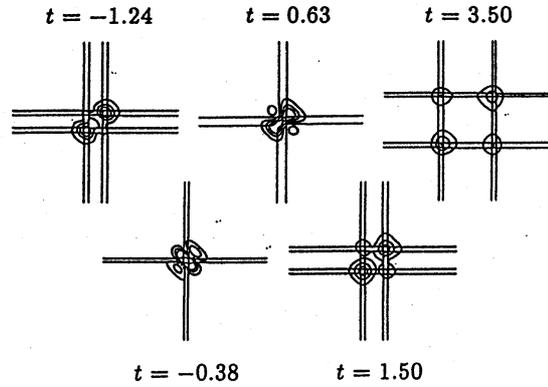
Fig.1

Solid profiles of $|A|^2$ in the case of the collision with parameters $\gamma 1 = \gamma 2 = 3$, $k1_r = k2_r = l1_r = l2_r = 4/5$, $k1_i = l1_i = 5/8$, and $k2_i = l2_i = -5/8$ at (a)$t = -3.0$, (b)$t = -0.76$, (c)$t = 0.0$, (d)$t = 0.23$, (e)$t = 0.5$, (f)$t = 1.5$, (g)$t = 3.5$. After the collision, there appears four pulses and propagate almost stably.
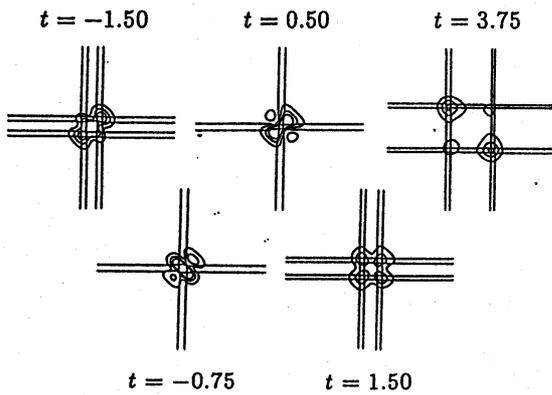
Fig. 2

$t = -1.00$ $t = 0.63$ $t = 3.00$

$t = -0.25$ $t = 1.12$

Contour Graphics of the collision of similar dromions with velocities $(k1_i, k2_i, l1_i, l2_i) = (6/8, -6/8, 6/8, -6/8)$. Contours are at 0.03, 0.1 and 0.2 for $|A|^2$, and, for U and V, 90% of the maximum values of them.

Fig. 3

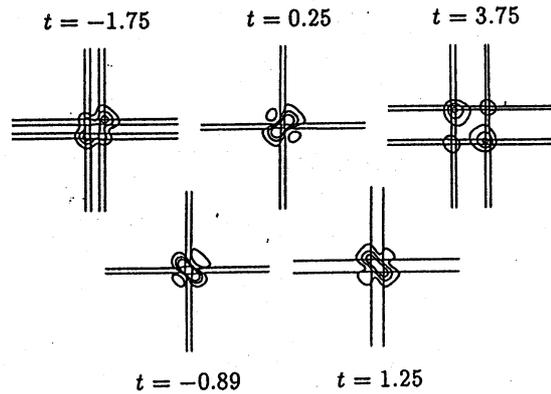$t = -1.24$ $t = 0.63$ $t = 3.50$

$t = -0.38$ $t = 1.50$

Contour Graphics of the collision of similar dromions with velocities $(k1_i, k2_i, l1_i, l2_i) = (5/8, -5/8, 5/8, -5/8)$. Contours are the same as fig.2.

Fig. 4

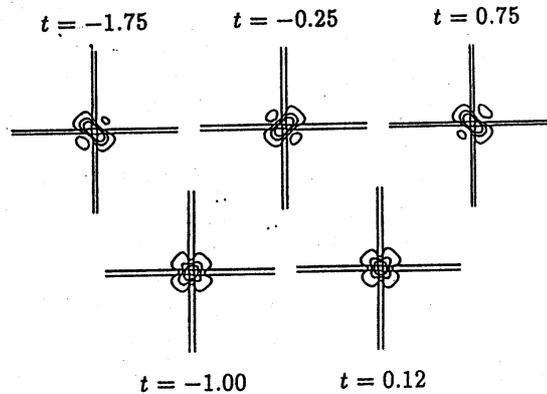$t = -1.50$ $t = 0.50$ $t = 3.75$

$t = -0.75$ $t = 1.50$

Contour Graphics of the collision of similar dromions with velocities $(k1_i, k2_i, l1_i, l2_i) = (4/8, -4/8, 4/8, -4/8)$. Contours are the same as fig.2.

Fig. 5

$t = -1.75$ $t = 0.25$ $t = 3.75$

$t = -0.89$ $t = 1.25$

Contour Graphics of the collision of similar dromions with velocities $(k1_i, k2_i, l1_i, l2_i) = (3/8, -3/8, 3/8, -3/8)$. Contours are the same as fig.2

Fig. 6

$t = -1.75$ $t = -0.25$ $t = 0.75$

$t = -1.00$ $t = 0.12$

Contour Graphics of a period of the intermediate oscillations in the collision with velocities $(k1_i, k2_i, l1_i, l2_i) = (1/8, -1/8, 1/8, -1/8)$. Contours are the same as fig.2. The oscillation occurs four times in this case, and the half period is observed to be about $1 \sim 1.5$s.